Large eddy simulations of offshore wind turbine wakes for two floating platform types

H M Johlas,[1] L A Martínez-Tossas,[2] M A Lackner,[1] D P Schmidt[1] and M J Churchfield[2]

[1]University of Massachusetts Amherst, Dept. of Mechanical and Industrial Engineering, Amherst, MA, USA
[2]National Renewable Energy Laboratory, Golden, CO, USA

E-mail: hjohlas@umass.edu

Abstract. The growing prospect for large farms of floating offshore wind turbines requires a better understanding of wake effects for floating turbines. In this work, large eddy simulations with an actuator line model are used to study the wake of the NREL 5 MW reference turbine mounted on the OC3-UMaine spar and OC4-DeepCwind semi-submersible platforms. The simulations are carried out in the Simulator fOr Wind Farm Applications (SOWFA) coupled with OpenFAST for the platform and turbine motion. The wake location, deficit, and turbulence levels are compared for the two floating platforms and equivalent fixed-turbine cases. The effects of neutral versus stable atmospheric conditions are also compared. Most notably, floating-turbine wakes are deflected upwards compared to fixed-turbine wakes, because of mean platform pitch. The spar wake deflects upwards more than the semi-submersible, while the stable atmosphere increases this vertical deflection compared to the neutral. The time-varying rotor motions do not significantly affect the mid-to-far wake, though the stable atmosphere shows larger fixed-floating differences in horizontal wake fluctuations.

1 Introduction

Wind turbine wake effects can increase turbine loads and decrease power generation in wind farm arrays. Wakes of floating offshore wind turbines (FOWTs) are particularly complex because of additional rotor motion from the floating platform. A better understanding of FOWT wake physics allows for improved engineering wake models used in design. This study examines how downstream wake characteristics differ between fixed and floating turbines, and specifically how these differences depend on floating platform type and atmospheric stability.

FOWT wakes are difficult to model accurately, partially because of the coupled nature of FOWT rotor aerodynamics and platform motion. To meet this challenge, large eddy simulations (LES) coupled with reasonable platform motions are increasingly used to study FOWT rotor aerodynamics and wakes [1, 2, 3]. Existing studies examine how platform type affects FOWT loads and rotor aerodynamics (see [4, 5, 6, 7]) and how atmospheric stability affects onshore turbine wakes (see [8, 9, 10, 11]). However, the effects of platform type and atmospheric stability on FOWT wakes require further study, particularly in the mid-to-far wake.

In this work, a FOWT wake is simulated with high-fidelity LES in the Simulator fOr Wind Farm Applications (SOWFA), coupled to the turbine simulator OpenFAST using an actuator line model (ALM). Wake characteristics are compared among a fixed turbine, a spar FOWT, and a semi-submersible FOWT in neutral and stable atmospheres.

2 Simulation setup

The wake of a single FOWT is simulated in SOWFA [12], a computational fluid dynamics tool developed by the National Renewable Energy Laboratory (NREL), based on OpenFOAM v2.4. These wake simulations in SOWFA model the turbine rotor using an ALM, coupled with NREL's aeroelastic turbine modeling tool OpenFAST v2.1.0 [13] for the rotor and platform motion. The simulation workflow includes three main steps. First, SOWFA LES of a large domain with periodic lateral boundaries and no turbine develops the wind shear and turbulent structures in the atmospheric boundary layer. Second, this "precursor" LES is continued for additional time, producing time histories for inflow/outflow boundary conditions. Third, SOWFA LES of a smaller domain, which includes the turbine represented by an ALM coupled to OpenFAST, simulates the turbine wake using the initial condition and inflow/outflow boundary conditions generated by the precursor LES. Further model details are summarized in Johlas *et al.* [14].

For all simulations in this study, the average hub height wind speed is 8 m/s from the southwest, which is below the turbine's rated wind speed [15]. Unidirectional, irregular JONSWAP waves with a significant wave height of H_s=8 m and a peak spectral period of T_P=14 s are simulated using OpenFAST's HydroDyn module. The wave direction is misaligned with the wind direction by 25^o. These conditions are selected based on the authors' previous findings that below-rated wind speeds, large wave heights, and misaligned wind-wave directions accentuate wake differences between fixed and floating platforms [14]. In this work, two floating platform types and two atmospheric stabilities are simulated.

2.1 Platform types

This study simulates the NREL 5 MW reference turbine (diameter D=126 m, hub height z=90 m, rated wind speed 11.4 m/s, and shaft tilt 5^o) [15] mounted on two floating platforms: the OC3-UMaine spar [4] and the OC4-DeepCWind semi-submersible [16]. The OC3-UMaine spar is identical to the OC3-Hywind spar [17], but with the catenary mooring lines adjusted to match the semi-sub's water depth of 200 m [4]. For comparison, a fixed turbine is also simulated by disabling the spar's platform motion and wave loading. Figure 1 shows the three platform types.

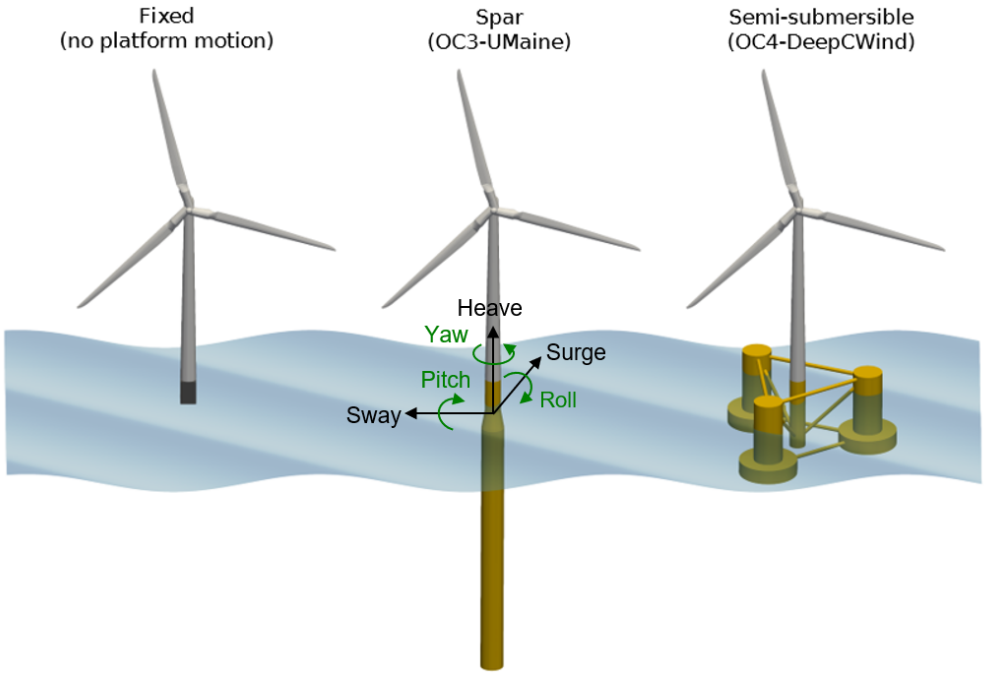

Figure 1. The NREL 5 MW reference turbine mounted on a fixed platform (left), the OC3-UMaine/OC3-Hywind spar (center), and the OC4-DeepCWind semi-submersible (right).

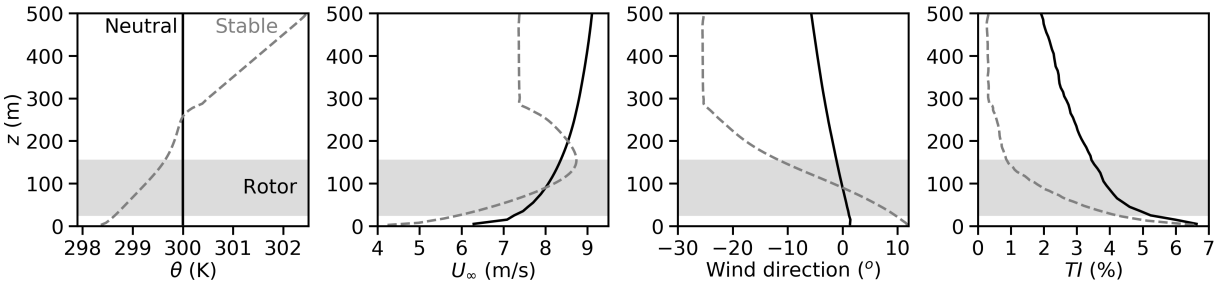

Figure 2. Potential temperature, wind speed, wind direction, and turbulence intensity plotted against elevation for neutral (−) and stable (−−) atmosphere simulations, averaged over time and across the domain. The shaded region indicates the rotor disc elevation.

2.2 Neutral atmosphere

First, a neutral atmosphere is simulated with no surface cooling and a strong capping inversion at an elevation of z=750 m. The surface roughness height is based on the Charnock model with α=0.011, as recommended by International Electrotechnical Commission standard 614000-3 [18]. The neutral precursor simulation develops the atmospheric boundary layer turbulence and wind profile over 5.5 hours in a 3 km by 3 km by 1.02 km domain at 10 m mesh resolution. Figure 2 shows the vertical profiles of the potential temperature θ, free stream horizontal wind speed U_∞, free stream horizontal wind direction, and turbulence intensity (TI), averaged over time and across the domain. The simulated neutral atmosphere profiles are shown by solid black lines in figure 2; the full vertical extent of the neutral profiles is presented in Johlas *et al.* [14].

When simulating the turbine in this neutral atmosphere, the computational domain is 2 km by 1 km by 1.02 km, with a base cell size of 10 m. A wake refinement region at 2.5 m resolution extends from $4D$ upstream to $10.3D$ downstream of the turbine, and a rotor refinement region at 1.25 m resolution extends from $0.5D$ upstream to $1.5D$ downstream. The rotor, wake, and base resolutions are comparable to those used in other SOWFA studies [1, 11, 19, 20, 21]. For these simulations in particular, halving the cell size in the wake refinement region has negligible effects on the floating turbine wakes, although small changes in the resolved turbulent kinetic energy are observed.

2.3 Stable atmosphere

A stable atmosphere is also simulated with a surface cooling rate of 0.25 K/h and an initial temperature inversion starting at z=250 m, based on the canonical GABLS1 case, as described by Beare *et al.* [22] but with the initial inversion raised above the rotor disc. The surface roughness height is identical to the neutral atmosphere simulation. The precursor simulation develops the stable atmosphere profiles shown in figure 2 (dashed grey lines) over 10 hours in a 2 km by 2 km by 0.5 km domain at 5 m mesh resolution. As shown in figure 2, the stable atmosphere exhibits higher wind shear, higher wind veer, and lower turbulence intensity across the rotor disc than the neutral atmosphere.

When simulating the turbine in this stable atmosphere, the computational domain is 2 km by 1 km by 0.5 km, with a base cell size of 5 m. The wake refinement and rotor refinement regions are the same as for the neutral turbine simulations. In total, the neutral and stable turbine simulation cell counts are 18.3 and 23.8 million cells, respectively.

3 Results

To understand how floating platform type affects downstream wake characteristics, all three platform types (fixed, spar, and semi-sub) are compared for the neutral atmosphere. To examine the effects of atmospheric stability, fixed and spar turbines are simulated in a stable atmosphere and then compared to the corresponding neutral atmosphere results. The wake and turbine behavior are examined over one hour, after discarding the initial 10 minutes of transient behavior.

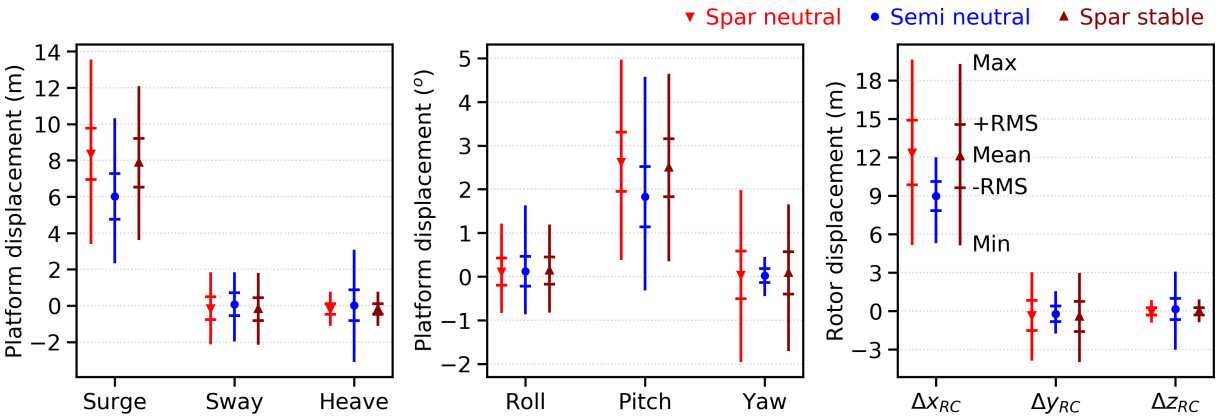

Figure 3. Floating turbine displacements for spar neutral (▼), semi-submersible neutral (●), and spar stable (▲) cases. The mean (symbols), root-mean-square (−), and minimum/maximum (vertical lines) are shown for six platform motions as well as rotor center displacements.

3.1 Floating platform motions

The nuances of platform motion are key to understanding how floating platforms affect wakes. In addition to the inherent time-varying motion, nonzero mean displacements of floating platforms also affect the wake. Figure 3 shows displacements in all six platform degrees of freedom (surge, sway, heave, roll, pitch, and yaw; see figure 1) and rotor center displacements (Δx_{RC}, Δy_{RC}, Δz_{RC}). For each floating case, the time-averaged displacement is reported alongside the root-mean-square (RMS), minimum, and maximum of the displacement time history.

Comparing the spar to the semi-sub (for a neutral atmosphere) in figure 3, the spar exhibits a larger mean surge, larger mean pitch, larger yaw RMS, and smaller heave RMS than the semi-sub. Although the spar and semi-sub have similar surge and pitch RMS, the phasing of these motions differs significantly between the two platforms. Surge and pitch are in phase for the spar but out of phase for the semi-sub, so that the spar Δx_{RC} RMS is more than twice the semi-sub RMS. The spar and semi-sub also have similar sway and roll RMS values, but the spar's larger yaw RMS causes a larger Δy_{RC} RMS because the rotor center is offset from the yaw axis. The spar's smaller heave RMS translates directly into smaller Δz_{RC} RMS.

Comparing the neutral atmosphere to the stable atmosphere (for the spar) in figure 3, the stable atmosphere creates slightly smaller RMS variations in most degrees of freedom, as expected for the stable atmosphere's lower turbulence intensity. The neutral mean surge and pitch are slightly larger than the stable mean values, but the mean displacements are generally similar between the neutral and stable atmospheres. The overall similarity in platform displacements between the neutral and stable atmospheres indicates that atmospheric stability plays little role in platform motion for these conditions.

3.2 Wake profiles

Wakes are characterized by a streamwise velocity deficit, $U_d = U(z) - U_\infty(z)$, and increased turbulent kinetic energy (TKE). Figure 4 shows U_d versus elevation z at different downstream locations for the fixed, spar, and semi-sub turbines in neutral (A) and stable (B) atmospheres. For each simulation, the downstream location x' is measured from the turbine's mean rotor center displacement such that $x' = x - \Delta x_{RC}$. Similarly, figure 5 plots the resolved TKE against elevation z at different downstream locations x'.

As shown in figures 4–5, all wakes recover with downstream distance as expected, indicated by reduced wake deficits and turbulence levels. The double-peak wake shape at $x'/D = 1, 3$ is caused by the low-thrust region near the blade roots. Figures 4–5 also show that the fixed-turbine wakes are similar to the floating-turbine wakes for both neutral and stable atmospheres.

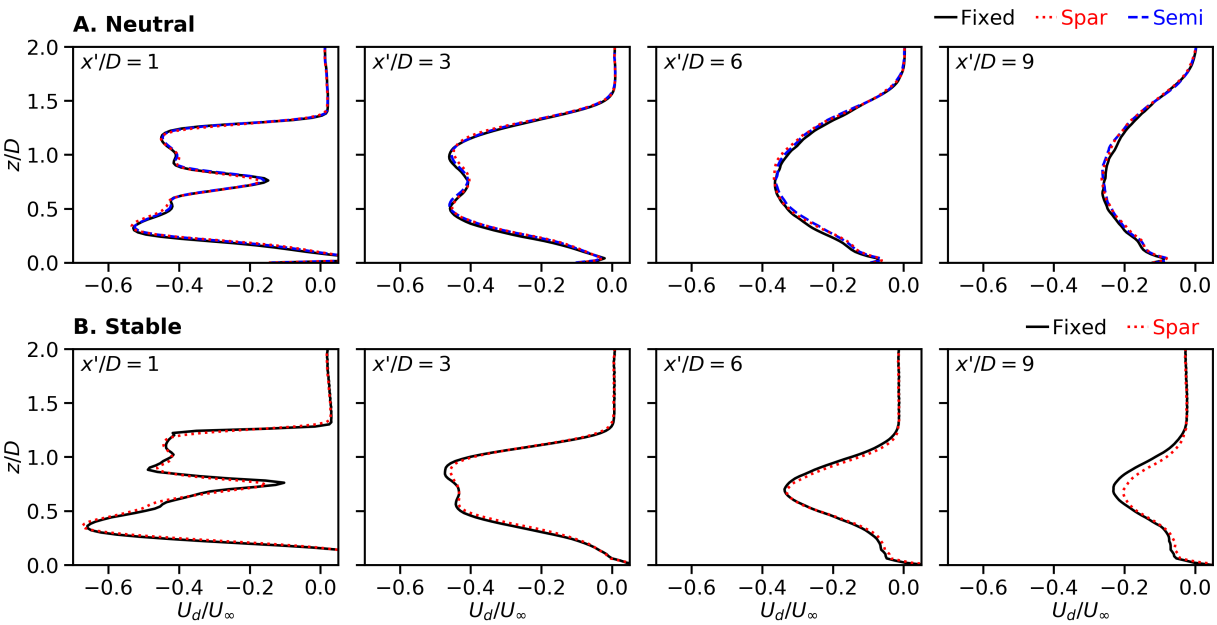

Figure 4. Time-averaged velocity deficit plotted against elevation at several downstream locations. Fixed and floating turbines are compared in neutral (A) and stable (B) atmospheres. The downstream locations are measured from the mean rotor displacement.

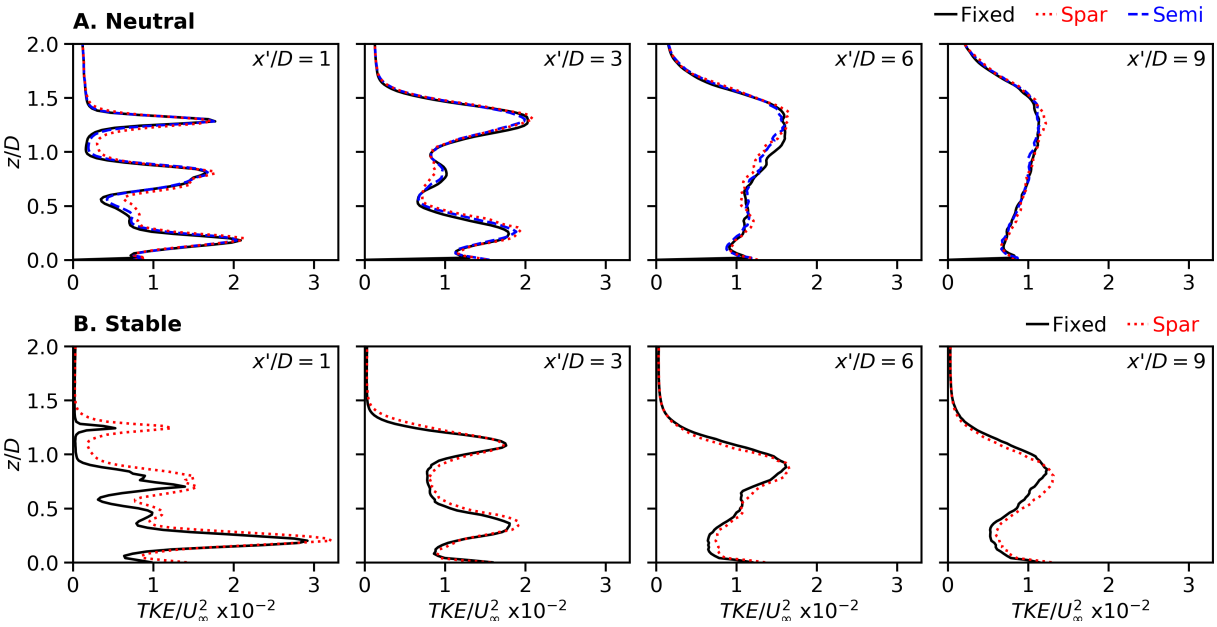

Figure 5. Turbulent kinetic energy plotted against elevation at several downstream locations. Fixed and floating turbines are compared in neutral (A) and stable (B) atmospheres. The downstream locations are measured from the mean rotor displacement.

3.3 Wake velocity differences

To better illustrate the small differences between the fixed-turbine wakes and floating-turbine wakes, figure 6 displays contours of the difference in time-averaged streamwise velocity, ΔU, at several cross-stream planes. Specifically, velocity differences are shown: between the spar and the fixed turbine in the neutral atmosphere (top), between the semi-sub and the fixed turbine in the neutral atmosphere (center), and between the spar and the fixed turbine in the stable

atmosphere (bottom). The downstream locations x' are again measured from the mean rotor displacement, and an outline of the undisplaced rotor disc is included for reference.

The most prominent feature of the time-averaged velocity difference contours in figure 6 is the positive ΔU near the bottom of the wake paired with a negative ΔU near the top of the wake. This is caused by the floating-turbine wakes deflecting upward compared to the fixed-turbine wakes: the floating wake is shifted upwards, creating a higher-velocity region near the bottom of the rotor disc and a lower-velocity region near the top. At x'/D = 1 and 3, the alternating positive-negative ΔU areas inside the rotor outline are caused by the upwards deflection of the double-peak wake shape shown in figures 4–5. The differences between the semi-sub and the fixed turbine are smaller than between the spar and the fixed turbine, although the same upwards deflection appears for both floating platforms. For the stable simulations, the higher wind veer skews the wake more, causing the positive-negative ΔU pattern to be stretched diagonally.

This upwards deflection of floating-turbine wakes is caused by the mean platform pitch backwards, creating a vertically curled wake, as also observed by Lee *et al.* [1] and Rockel *et al.* [23]. This curled wake resulting from platform pitch is similar to curled wakes caused by rotor tilt [24, 25, 20, 21], and is also analogous to horizontally curled wakes caused by nacelle yaw. Although the vertical deflection is measurable for these floating-turbine wakes, the curled shape distortion is relatively weak because of the low effective rotor tilt angles (5^o shaft tilt plus 1-3^o mean platform pitch), especially beyond the near wake, $x'/D > 1$.

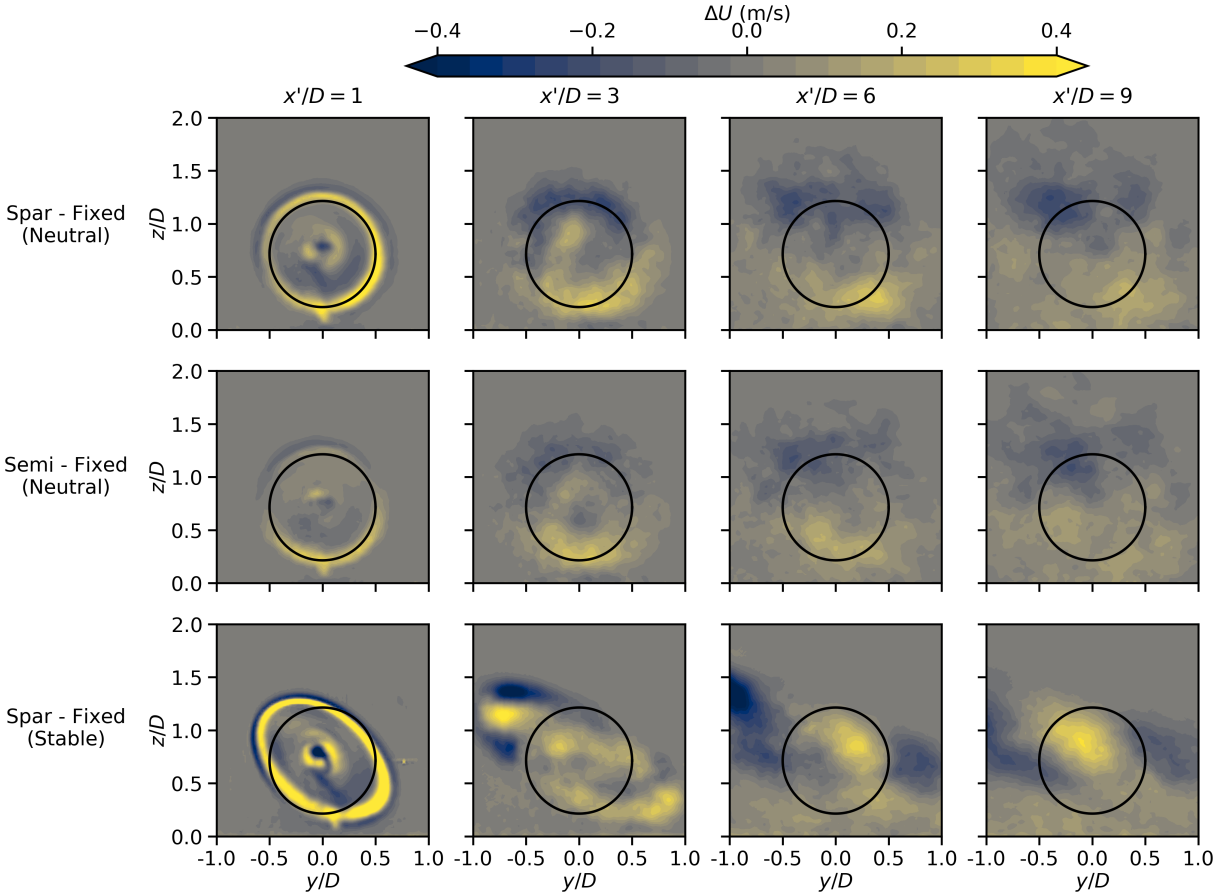

Figure 6. Differences in time-averaged wake velocity between fixed and floating simulations at downstream locations of $x'/D = 1, 3, 6, 9$. The downstream locations are measured from the mean rotor displacement. The undisplaced rotor disc is outlined for reference.

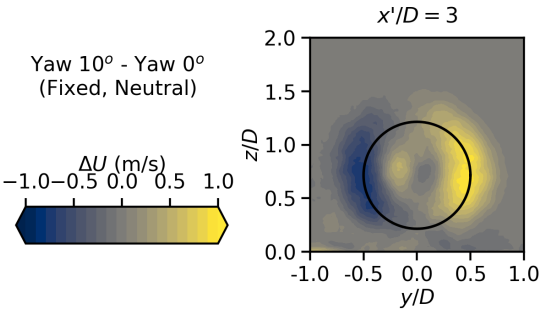

Figure 7. Differences in time-averaged wake velocity between a fixed turbine with 10^o rotor yaw and a fixed turbine with 0^o rotor yaw, at a downstream location of $x'/D = 3$. The undisplaced rotor disc is also outlined.

To further illustrate the reason why floating-turbine wakes are deflected upward compared to fixed-turbine wakes, figure 7 shows a contour at $x'/D = 3$ of the difference in time-averaged streamwise velocity ΔU between a fixed turbine with a 10^o nacelle yaw angle and a fixed turbine with a 0^o yaw angle in the neutral atmosphere. The horizontal positive-negative ΔU pattern in figure 7 is similar to the vertical positive-negative ΔU in figure 6, including the effects of the double-peak wake shape inside the rotor outline. This similarity to the wake differences between two fixed turbines (one yawed and one without yaw) suggests that the floating-turbine wakes' upward deflection is mostly caused by the mean platform pitch displacement, rather than any time-varying motions associated with the floating platform.

In contrast to the time-averaged wake velocity differences in figure 6, the instantaneous wake velocity differences between the floating and fixed turbines (not shown) do not show recognizable patterns over time or space. Although the instantaneous streamwise velocity in the wake is noticeably different (1-2 m/s) at any given time between the fixed and floating simulations, these differences represent a different realization of wake turbulence and do not form spatial or temporal patterns that would affect a downstream turbine.

3.4 Wake centers

To further investigate how floating-turbine wakes differ from fixed-turbine wakes, the wake center is tracked over time. The wake center at each downstream location is identified every 1 s, using the SAMWICH toolbox [26] by fitting a 2D Gaussian to the streamwise velocity deficit and taking the Gaussian center as the wake center. This method can track the wake center up to $x'/D = 6$, but results farther downstream are omitted because of spurious wake center locations.

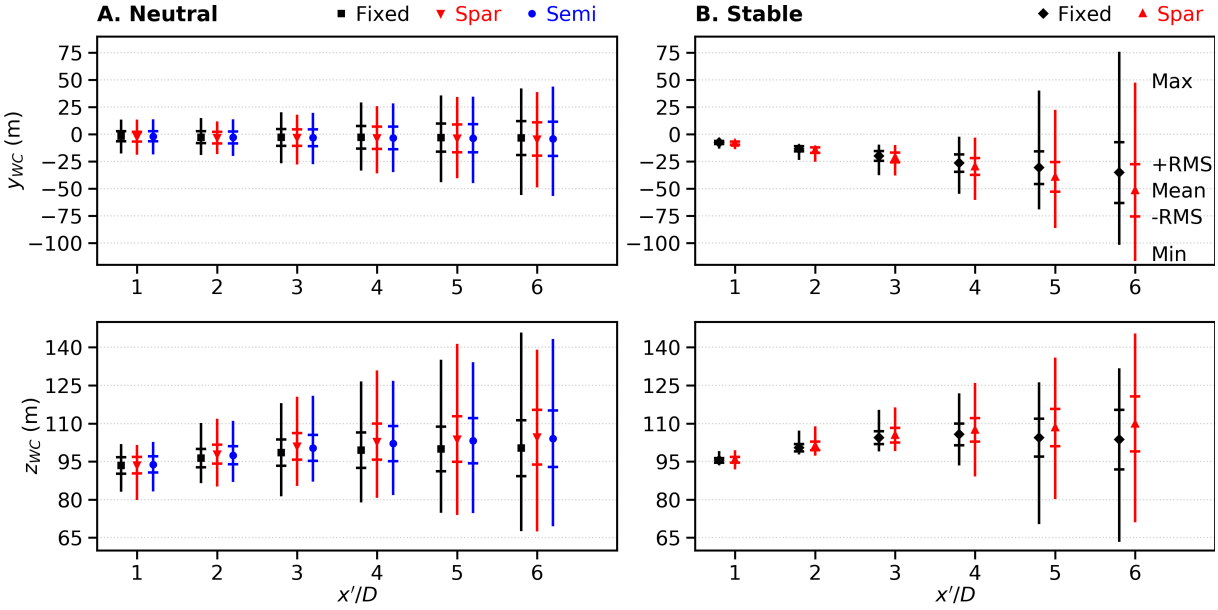

Figure 8. Wake center coordinates y_{WC}, z_{WC} versus downstream location in neutral (A) and stable (B) atmospheres. The mean (symbols), root-mean-square (−), and minimum/maximum (|) are shown for the fixed (■, ◆), spar (▼, ▲), and semi-submersible (●) platforms.

Figure 8 shows the wake center cross-stream coordinate y_{WC} and vertical coordinate z_{WC} at different downstream slices x' for each platform type in neutral (A) and stable (B) atmospheres. The time-averaged wake center is shown with the RMS, minimum, and maximum of the wake center time history. The downstream location x' is measured from the mean rotor displacement.

The mean wake center elevations z_{WC} in figure 8 confirm that the floating-turbine wakes are deflected upwards, compared to the fixed-turbine wakes. However, even the fixed turbine wakes are somewhat deflected upward, due to the 5^o shaft tilt [15]. The spar wake center is deflected upward more than the semi-sub wake center, which is consistent with the spar's larger wake velocity differences in figure 6. This trend is caused by the spar's larger mean platform pitch (see figure 3). Comparing atmospheric stabilities, the stable spar wake is deflected more than the neutral spar, suggesting that floating-turbine wake deflection is influenced by wind shear.

The mean wake center cross-stream locations y_{WC} in figure 8 are generally similar between fixed and floating turbines for the neutral atmosphere, with differences less than $1\%D$. Since the stable atmosphere has higher wind veer, the stable wakes are deflected more than the neutral wakes in the cross-stream direction. Furthermore, the stable floating-turbine wakes are deflected more in the cross-stream direction than the stable fixed-turbine wakes (up to $13\%D$). This is caused by the vertical wake deflection interacting with the stable atmosphere's wind veer.

The time-varying fluctuations in wake center location in figure 8 are generally similar between the fixed and floating turbines. For both y_{WC} and z_{WC}, the RMS differences between fixed and floating wake center locations are mostly less than $1\%D$. However, the stable atmosphere's low TI increases the importance of the platform motion's effect on the wake, creating a $3\%D$ difference in horizontal RMS between the stable fixed and floating cases at $x'/D = 6$. Differences in the RMS y_{WC} and z_{WC} between the stable and neutral atmospheres are generally larger than the RMS differences between fixed and floating turbines, indicating that atmospheric flow influences wake center variations more than floating platform motion.

Table 1. Differences in mean and root-mean-square values between floating and fixed turbines. Differences are shown for key platform motions; rotor center displacements; and wake center locations at three downstream locations.

	Spar − Fixed (Neutral)		Semi − Fixed (Neutral)		Spar − Fixed (Stable)	
Difference	Mean	RMS	Mean	RMS	Mean	RMS
Surge (m)	8.36	1.41	6.02	1.26	7.87	1.34
Heave (m)	−0.19	0.29	0.02	0.85	−0.18	0.29
Pitch (^{o})	2.63	0.68	1.83	0.69	2.49	0.66
Yaw (^{o})	0.04	0.55	0.03	0.16	0.08	0.49
Δx_{RC} (m)	12.21	2.52	8.82	1.12	11.92	2.46
Δy_{RC} (m)	−0.33	1.16	−0.20	0.58	−0.41	1.15
Δz_{RC} (m)	−0.05	0.26	0.13	0.81	−0.05	0.26
y_{WC} at x'/D=1	$-0.37\%D$	$-0.03\%D$	$-0.11\%D$	$-0.01\%D$	$-0.45\%D$	$0.00\%D$
y_{WC} at x'/D=3	$-0.20\%D$	$-0.01\%D$	$-0.25\%D$	$-0.05\%D$	$-1.17\%D$	$0.04\%D$
y_{WC} at x'/D=6	$-0.70\%D$	$-0.30\%D$	$-0.67\%D$	$0.03\%D$	$-12.97\%D$	$-3.05\%D$
z_{WC} at x'/D=1	$0.12\%D$	$0.04\%D$	$0.30\%D$	$-0.04\%D$	$0.21\%D$	$0.18\%D$
z_{WC} at x'/D=3	$1.96\%D$	$0.03\%D$	$1.47\%D$	$-0.03\%D$	$0.77\%D$	$0.33\%D$
z_{WC} at x'/D=6	$3.42\%D$	$-0.16\%D$	$2.95\%D$	$0.08\%D$	$4.93\%D$	$-0.66\%D$

3.5 Summary of floating-fixed differences

Table 1 summarizes the key differences between fixed and floating turbines presented in figures 3–8, illustrating how floating platform motion and rotor center displacements translate into differences in wake center locations. As indicated in table 1, mean platform pitch values of 1.8-2.6^o result in increased vertical wake deflections of 3-5%D at x'/D=6, with the stable atmosphere increasing the vertical wake deflection. Increased rotor displacement RMS values of 1-3 m result in negligible (mostly less than 1%D) changes in wake center location RMS, though the stable atmosphere creates larger differences (up to 3%D) in horizontal wake center fluctuations between the fixed and floating cases.

4 Conclusions

Overall, floating-turbine wakes have similar characteristics to fixed-turbine wakes, except that floating-turbine wakes are deflected upwards because of mean platform pitch (see figures 4–8). This vertical wake deflection for floating turbines is similar to horizontal wake deflection caused by nacelle yaw in fixed turbines (see figure 7). The spar platform produces larger upwards wake deflections than the semi-sub, because of the spar's larger mean platform pitch (see table 1). The stable atmosphere produces larger vertical and horizontal deflections than the neutral atmosphere (see table 1), indicating that wind shear and wind veer interact with this pitch-driven wake deflection.

Floating-turbine wake fluctuations in time do not significantly differ from fixed-turbine wake fluctuations, even for conditions selected to accentuate floating wake differences (high wave height, below-rated wind speed, and wind-wave misalignment). The RMS fluctuations in wake center location differ by less than 1%D between fixed and floating turbines in most cases, although the stable atmosphere's low turbulence intensity allows the floating platform motion to have a larger effect on horizontal wake center fluctuations (see figure 8 and table 1).

These findings suggest that reduced-order wake models for fixed turbines can reasonably apply to floating-turbine wakes, especially curled wake models that capture upwards wake deflection caused by mean platform pitch. Adjustments may be necessary for vertical wake deflections interacting with wind shear and wind veer. Future work includes comparing these LES results to reduced-order wake models, as well as investigating downstream FOWT loads and power when placed in the wake.

Acknowledgments

The authors thank Jason Jonkman and Amy Robertson of NREL for their advice on this work. This study is supported by a National Science Foundation Graduate Research Fellowship, grant #1451512. This work used the Extreme Science and Engineering Discovery Environment (XSEDE) funded by National Science Foundation grant #ACI-1548562, as well as National Renewable Energy Laboratory computational resources sponsored by the U.S. Department of Energy Office of Energy Efficiency and Renewable Energy. This work was authored in part by the National Renewable Energy Laboratory, operated by Alliance for Sustainable Energy, LLC, for the U.S. Department of Energy (DOE) under Contract No. DE-AC36-08GO28308. Funding provided by the U.S Department of Energy Office of Energy Efficiency and Renewable Energy Wind Energy Technologies Office. The views expressed in the article do not necessarily represent the views of the DOE or the U.S. Government. The U.S. Government retains and the publisher, by accepting the article for publication, acknowledges that the U.S. Government retains a nonexclusive, paid-up, irrevocable, worldwide license to publish or reproduce the published form of this work, or allow others to do so, for U.S. Government purposes.

References

[1] Lee S, Churchfield M, Driscoll F, Sirnivas S, Jonkman J, Moriarty P, Skaare B, Nielsen F and Byklum E 2018 *Energies* **11**(7) 1895
[2] Wang J, Wang C, Castañeda O D, Campagnolo F and Bottasso C L 2018 *J. Phys.: Conf. Ser.* **1037** 072032

[3] Liu Y, Xiao Q, Incecik A and Peyrard C 2019 *Wind Energy* **22** 1–20
[4] Robertson A N and Jonkman J M 2011 *Proc. of the 21st Int. Offshore and Polar Engineering Conf. (Maui)* ISOPE-I-11-204
[5] Sebastian T and Lackner M 2013 *Wind Energy* **16** 339–52
[6] Bachynski E E, Kvittem M I, Luan C and Moan T 2014 *J. Offshore Mech. Arct. Eng.* **136** 041902
[7] Sebastian T and Lackner M 2012 *Energies* **5**(4) 968–1000
[8] Xie S and Archer C L 2017 *Boundary Layer Meteorol.* **165** 87–112
[9] Abkar M and Porté-Agel F 2015 *Phys. Fluids* **27** 035104
[10] Wu Y T and Porté-Agel F 2012 *Energies* **5**(12) 5340–62
[11] Churchfield M J, Lee S, Michalakes J and Moriarty P J 2012 *J. Turbul.* **13** N14
[12] Churchfield M and Lee S 2015 NWTC information portal: SOWFA (National Renewable Energy Laboratory) URL `https://nwtc.nrel.gov/SOWFA`
[13] Jonkman J and Sprague M 2019 NWTC information portal: OpenFAST (National Renewable Energy Laboratory) URL `https://nwtc.nrel.gov/OpenFAST`
[14] Johlas H M, Martínez-Tossas L A, Schmidt D P, Lackner M A and Churchfield M J 2019 *J. Phys.: Conf. Ser.* **1256** 012018
[15] Jonkman J, Butterfield S, Musial W and Scott G 2009 *National Renewable Energy Laboratory Report* NREL/TP-500-38060
[16] Robertson A, Jonkman J, Masciola M, Song H, Goupee A, Coulling A and Luan C 2014 *National Renewable Energy Laboratory Report* NREL/TP-5000-60601
[17] Jonkman J 2010 *National Renewable Energy Laboratory Report* NREL/TP-500-47535
[18] International Electrotechnical Commission 2009 *IEC 61400-3 Wind Turbines – Part 3: Design Requirements for Offshore Wind Turbines*
[19] Martínez-Tossas L A, Churchfield M J and Leonardi S 2015 *Wind Energy* **18** 1047–60
[20] Fleming P, Gebraad P M, Lee S, van Wingerden J W, Johnson K, Churchfield M, Michalakes J, Spalart P and Moriarty P 2015 *Wind Energy* **18** 2135–43
[21] Fleming P A, Gebraad P M, Lee S, van Wingerden J W, Johnson K, Churchfield M, Michalakes J, Spalart P and Moriarty P 2014 *Renewable Energy* **70** 211–8
[22] Beare, R J *et al* 2006 *Boundary Layer Meteorol.* **118** 247–72
[23] Rockel S, Peinke J, Hölling M and Cal R B 2017 *Renewable Energy* **112** 1–16
[24] Annoni J, Scholbrock A, Churchfield M and Fleming P 2017 *American Control Conf. (Seattle)* pp 717–22
[25] Weipao M, Chun L, Jun Y, Yang Y and Xiaoyun X 2016 *J. Solar Energy Eng.* **138** 034501
[26] Eliot Q 2019 SAMWICH Box: Simulated And Measured Wake Identification and CHaracterization Toolbox URL `https://github.com/ewquon/waketracking`